Journal of Materials Chemistry C

PAPER

View Article Online
View Journal

Published on 07 November 2016. Downloaded by Synchrotron Radiation Library on 23/11/2016 03:23:59.

Cite this: DOI: 10.1039/c6tc04300c

Synthesis, molecular and photovoltaic/transistor properties of heptacyclic ladder-type di(thienobenzo)fluorene-based copolymers†

Chia-Hao Lee,[a] Yu-Ying Lai,[ab] Fong-Yi Cao,[a] Jhih-Yang Hsu,[a] Zong-Liang Lin,[a] U-Ser Jeng,[cd] Chun-Jen Su[c] and Yen-Ju Cheng*[a]

Received 4th October 2016,
Accepted 18th October 2016

DOI: 10.1039/c6tc04300c

www.rsc.org/MaterialsC

We present a facile synthesis method to make a new ladder-type heptacyclic dithienobenzofluorene (**DTBF**) framework, where the central 2,7-fluorene unit is covalently fastened with two external thiophenes *via* two C=C bridges. A dieneyne-containing precursor undergoes DBU-induced double benzannulation to regiospecifically introduce two solubilizing 2-octyldodecyl side chains at 5,10-positions of **DTBF**. The rigid and coplanar **Br-DTBF** monomer with sufficient solubility was copolymerized with 5,6-difluoro-4,7-bis(5-(trimethylstannyl)thiophen-2-yl)benzo[*c*][1,2,5]thiadiazole (**Sn-DTFBT**) and 5,10-bis(5-(trimethylstannyl)thiophen-2-yl)naphtho[1,2-*c*:5,6-*c*']bis([1,2,5]thiadiazole) (**Sn-DTNT**) *via* Stille coupling to furnish two donor–acceptor copolymers, **PDTBFFBT** and **PDTBFNT**, respectively. Their thermal, optical, electrochemical, molecular stacking and photovoltaic properties are investigated. **PDTBFNT** has a higher molecular weight, smaller optical and electrochemical band gaps, and stronger solid-state packing than **PDTBFFBT**. DFT calculations were carried out to gain insight into the electronic and structural properties of **DTBF** and its derivatives. Bulk heterojunction solar devices with the ITO/ZnO/polymers:$PC_{71}BM$/MoO_3/Ag configuration were fabricated. By adding 5 vol% diphenyl ether (DPE) as an additive, **PDTBFNT**:$PC_{71}BM$ and **PDTBFFBT**:$PC_{71}BM$ devices achieved the power conversion efficiencies of 5.22% and 2.68%, respectively. The superior efficiency of **PDTBFNT** over **PDTBFFBT** is attributed to the better LUMO energy alignment between **PDTBFNT** and $PC_{71}BM$ and the face-on π-stacking of **PDTBFNT** in the active layer. Moreover, **PDTBFNT** exhibited a higher field-effect transistor hole mobility of 1.90 × 10^{-2} cm^2 V^{-1} s^{-1} than **PDTBFFBT** with a value of 3.96 × 10^{-3} cm^2 V^{-1} s^{-1}.

Introduction

The field of organic optoelectronics has been advanced drastically by the expansion of p-type and n-type semiconductor libraries.[1] In particular, polymer solar cells (PSCs) benefit substantially from the development of p-type conjugated polymers.[2] It has been documented that enhancing the planarity of polyaromatic systems is advantageous to π-electron delocalization, which can further extend the effective conjugation length and reduce the optical band gap to allow for capturing more photons of the solar spectrum.[3] Moreover, the increase of structural rigidity can lower the rotational disorder and diminish the reorganization energy, thus improving the intrinsic charge mobility.[4] The tricyclic 2,7-fluorene unit is a useful electron-rich building block for preparing various p-type polymers due to its deep-lying HOMO energy levels and good hole-transporting properties to achieve high open-circuit voltages (V_{oc}) and short circuit currents (J_{sc}).[5] Therefore, embedding a fluorene motif into a ladder-type π-conjugated framework would be an attractive and promising molecular design for developing new semiconductors.[6] For example, based on a 2,7-dithienylfluorene skeleton, we recently develop a synthetic method to fasten the central fluorene and two external thiophenes by two sp^3–carbon bridges, forming a heptacyclic ladder-type structure called dithienocyclopentafluorene (**DTCF**, Scheme 1).[6c,d] The solar cell device incorporating a poly(dithienocyclopentafluorene-*alt*-benzothiadiazole) (**PDTCFBT**) polymer has shown better performance than that of its open-chain counterpart.[6c,d,7] Despite the fact that the conjugated backbones are highly planar, the two geminal side chains on the tetrahedron sp^3-hybridized carbons will stick out of the conjugated plane and thus inevitably impose certain steric

[a] Department of Applied Chemistry, National Chiao Tung University, 1001 University Road, Hsin-Chu, 30010, Taiwan. E-mail: yjcheng@mail.nctu.edu.tw
[b] Institute of Polymer Science and Engineering, National Taiwan University, Taipei, 10617, Taiwan
[c] National Synchrotron Radiation Research Center, 101 Hsin-Ann Road, Hsin-Chu Science Park, Hsin-Chu 30076, Taiwan
[d] Department of Chemical Engineering, National Tsing Hua University, Hsinchu 30013, Taiwan

† Electronic supplementary information (ESI) available. See DOI: 10.1039/c6tc04300c

Published on 07 November 2016. Downloaded by Synchrotron Radiation Library on 23/11/2016 03:23:59.

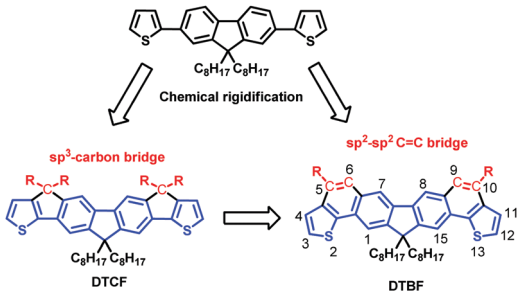

Scheme 1 Sp^3–Carbon-bridged and sp^2–sp^2 ethylene-bridged heptacyclic dithienocyclopentafluorene (**DTCF**) and dithienobenzofluorene (**DTBF**) Arenes.

hindrance to suppress intermolecular interactions. To circumvent this steric deficiency of sp^3-hybridized bridges, it is of interest to covalently fasten the central fluorene and two outer thiophene rings by sp^2–sp^2 C=C ethylene bridges with concomitant formation of two embedded benzene rings, resulting in a new heptacyclic ladder-type structure denoted as dithienobenzofluorene (**DTBF**) (Scheme 1). Forming benzene rings is also advantageous to lower the HOMO energy level of **DTBF** for obtaining higher V_{oc}. Nevertheless, introducing aliphatic side chains on the sp^2–sp^2 C=C moieties of this highly planarized **DTBF** is imperative to ensure solubility but synthetically challenging. In this research, we first successfully synthesized a **DTBF** with two 2-octyldodecyl chains regiospecifically at its 5,10 positions. The key step to construct the **DTBF** is *via* double base-induced benzannulation of a dieneyne-based precursor.[8] 5,6-Difluorobenzo[*c*][1,2,5]thiadiazole (FBT) has been used extensively as an electron acceptor to construct conjugated polymers for applications in organic optoelectronics.[8e,9] Naphtho[1,2-*c*:5,6-*c*′]bis([1,2,5]-thiadiazole) NT, an emerging electron acceptor, has also led to high-performance p-type polymers in PSCs.[10] Consequently, the brominated **DTBF** monomer was copolymerized with 5,6-difluoro-4,7-bis(5-(trimethylstannyl)thiophen-2-yl)benzo[*c*][1,2,5]thiadiazole (**Sn-DTFBT**) and 5,10-bis(5-(trimethylstannyl)thiophen-2-yl)naphtho-[1,2-*c*:5,6-*c*′]bis([1,2,5]thiadiazole) (**Sn-DTNT**) *via* Pd-catalyzed Stille coupling to afford two donor–acceptor copolymers, **PDTBFFBT** and **PDTBFNT**, respectively. The thermal, optical, electrochemical, photovoltaic, and stacking properties and DFT calculations of **PDTBFFBT** and **PDTBFNT** are investigated and compared. The bulk heterojunction (BHJ) solar device using the **PDTBFNT**: $PC_{71}BM$ blend exhibited a decent efficiency of 5%, validating the promising capabilities of **DTBF** in the field of PSCs.

Results and discussion

Design and synthesis of Br-DTBF, PDTBFFBT, and PDTBFNT

The synthetic route of the monomer **Br-DTBF** is depicted in Scheme 2. Stille coupling of 3,6-dibromo-2,7-diiodo-9,9-dioctylfluorene (**1**) regioselectively occurred at the 2,7-positions to afford **2**. **3** was obtained by palladium-catalyzed Sonogashira coupling of **2** with 4-octyl-1-tetradecyne. 1,8-Diazabicycloundec-7-ene (DBU)-induced benzannulation of **3** led to the formation of **DTBF** with the two benzene rings embedded between the outer thiophenes and the central fluorene. This reaction involves isomerization of the propargyl moiety to an allene group followed by intramolecular 6π-electrocyclization/aromatization.[8] Bromination of **DTBF** by typical *N*-bromosuccinimide (NBS) failed to afford **Br-DTBF**, whereas lithiating **DTBF** followed by quenching with 1,2-dibromotetrachloroethane successfully generated **Br-DTBF**. As shown in Scheme 3, **Br-DTBF** was then copolymerized with the **Sn-DTFBT** and **Sn-DTNT** monomers to form **PDTBFFBT** and **PDTBFNT**, respectively.

Thermal properties and molecular weights

As determined by thermogravimetric analysis, thermal decomposition temperatures (T_d) of **PDTBFFBT** and **PDTBFNT** are estimated to be 382 °C and 325 °C, respectively (Fig. 1 and Table 1). Differential scanning calorimetry reveals that no detectable thermal transition was found for both polymers, indicating their amorphous character in the scanning temperature between 80 and 280 °C (Fig. S1, ESI†). The number-average molecular weight (M_n) and polydispersity index (PDI) determined by gel permeation chromatography were 7.8 K g mol^{-1} and 1.2 for **PDTBFFBT**, and 14.3 K g mol^{-1} and 3.4 for **PDTBFNT**. (Table 1).

Optical properties

The UV-vis absorption spectra of the two polymers in $CHCl_3$ and thin film are shown in Fig. 2 and the results are

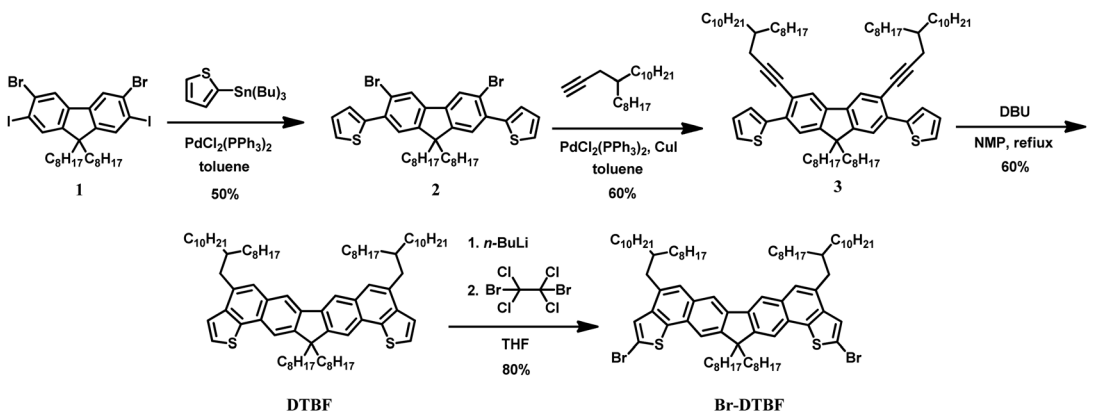

Scheme 2 Synthetic route toward **Br-DTBF**.

 This journal is © The Royal Society of Chemistry 2016

Published on 07 November 2016. Downloaded by Synchrotron Radiation Library on 23/11/2016 03:23:59.

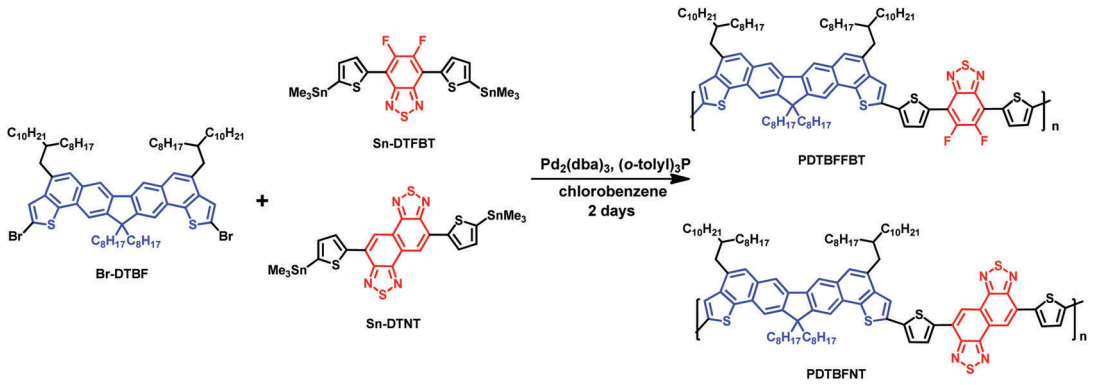

Scheme 3 Synthesis of the two D–A copolymers **PDTBFFBT** and **PDTBFNT**.

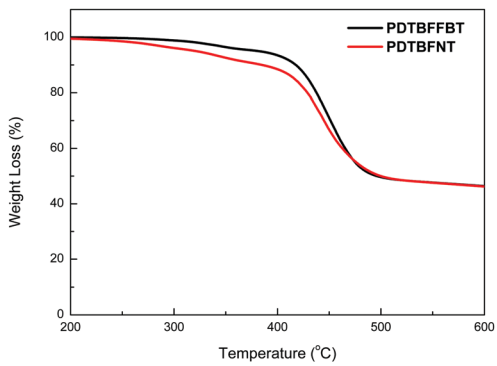

Fig. 1 Thermogravimetric analyses of **PDTBFFBT** and **PDTBFNT** at a ramping rate of 10 °C min^{-1}.

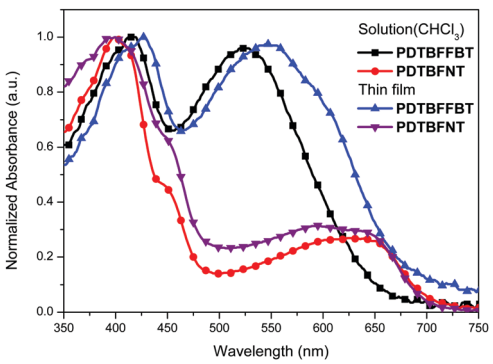

Fig. 2 Normalized UV-vis absorption spectra of **PDTBFFBT** and **PDTBFNT** in chloroform solutions and thin films.

summarized in Table 1. **PDTBFFBT** and **PDTBFNT** exhibit two major absorption bands in the solution and solid states. Based on the computational results (see Theoretical calculations), the longer wavelengths at 522 nm and 626 nm for **PDTBFFBT** and **PDTBFNT** are attributed to the intramolecular charge transfer (ICT) between the electron-rich and the electron-deficient segments. The optical band gap of **PDTBFNT** is smaller than that of **PDTBFFBT**, indicating that the accepting strength of NT is stronger than that of FBT, which is consistent with other studies.[11] The aggregation-induced red-shift in thin film is much more pronounced for **PDTBFFBT** than **PDTBFNT**.

Electrochemical properties

Thin film cyclic voltammetry (CV) was employed to investigate the electrochemical properties and determine the highest occupied molecular orbital (HOMO) and lowest unoccupied molecular orbital (LUMO) energies of the polymers (Fig. 3 and Table 1). The LUMO energy levels of **PDTBFFBT** and **PDTBFNT** are determined to be −3.17 and −3.67 eV, respectively. It has been proposed that the energy required for exciton dissociation in organic materials is around 0.3 eV.[2a] The LUMO energy level of **PDTBFNT** is 0.33 eV higher than that of the $PC_{71}BM$ (−4.0 eV) acceptor, which is suitable for energetically favorable electron transfer. On the other hand, the much higher-lying LUMO energy level of **PDTBFFBT** may be detrimental to exciton dissociation, resulting in poor short-circuit current (J_{sc}). Both **PDTBFFBT** and **PDTBFNT** possess low-lying HOMO energy levels which are beneficial for attaining good ambient stability and higher V_{oc} (Table 1).

Theoretical calculations

It is envisioned that the alternation of the bridging linker from the tetrahedron carbon in **DTCF** to the ethylene unit in **DTBT**

Table 1 Summary of the intrinsic properties of **PDTBFFBT** and **PDTBFNT**

	M_n[a] (g mol^{-1})	PDI[b]	T_d[c] (°C)	E_g^{opt}[d] (eV)	E_g^{ele}[e] (eV)	λ_{max} (nm) $CHCl_3$	λ_{max} (nm) Film	E_{HOMO} (eV)	E_{LUMO} (eV)
PDTBFFBT	7.8 K	1.2	382	1.85	2.43	414, 522	426, 545	−5.60	−3.17
PDTBFNT	14.3 K	3.4	325	1.78	2.03	400, 626	400, 616	−5.70	−3.67

[a] M_n = number-average molar weight. [b] PDI = polydispersity index. [c] T_d = decomposition temperature at 5% weight loss. [d] E_g^{opt} was estimated from the onset of the UV spectrum in thin films. [e] E_g^{opt} was estimated from cyclic voltammetry.

Published on 07 November 2016. Downloaded by Synchrotron Radiation Library on 23/11/2016 03:23:59.

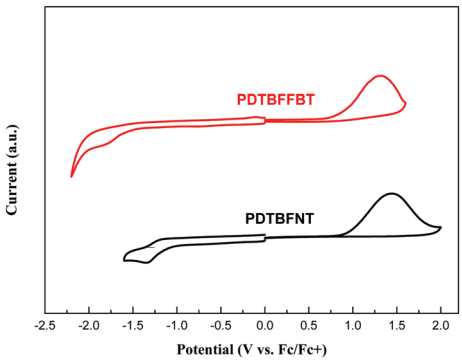

Fig. 3 Cyclic voltammograms of **PDTBFFBT** and **PDTBFNT** in thin films at a scan rate of 100 mV s^{-1}.

would change the molecular geometry and the intermolecular stacking. Quantum-chemical calculations with the Gaussian09 suite employing the B3LYP density functional in combination with the 6-311G(d,p) basis set were then employed to investigate the structural difference between **DTCF** and **DTBF**. The aliphatic side chains in **DTCF** and **DTBF** are all simplified due to the insignificant influence on the geometry of the conjugated system. The optimized geometries of **DTCF** and **DTBF** suggest that both molecules possess a high degree of planarity (Fig. 4). The most noticeable geometrical dissimilarity between **DTCF** and **DTBF** lies in the molecular curvature which can be quantified by the angle between two axes along the two outer thiophenes as shown in Fig. 4. **DTBF** and **DTCF** have angles of 68° and 154°, respectively, meaning that **DTBF** has a more curved backbone. The different molecular curvature and geometrical shapes can be used to modulate the molecular properties of the resultant conjugated polymers. Furthermore, with the intention of gaining insight into the electronic structures of **PDTBFFBT** and **PDTBFNT**, dimeric models of **2-DTBFFBT** and **2-DTBFNT** are adopted and geometry-optimized under the B3LYP/6-311G(d,p) level of theory. The side-chain substituents are simplified in order to reduce the computational time. The optimized geometries of **2-DTBFFBT** and **2-DTBFNT** are depicted in Fig. 5. Both model compounds exhibit quasi-planar and quasi-linear conjugated backbones. Time-dependent density functional calculations (TD-MPW1PW91/6-311G(d,p)) are then carried out by using the optimized geometries with solvation in chloroform by applying the polarizable continuum model. The results are summarized in Table 2 and the calculated HOMO and LUMO electron-density distributions are illustrated in Fig. 6. Although the deviation exists between the experimental observables and theoretical estimates, a qualitative agreement can be perceived. For instance, the computation results suggest that **2-DTBFFBT** and **2-DTBFNT** have comparable HOMO energy levels but the LUMO of **2-DTBFFBT** is higher than that of **2-DTBFNT**, which is consistent with the electrochemical results. The electron density of the HOMO is distributed along the central conjugated backbone of **2-DTBFFBT** and **2-DTBFNT**, while the electron density of the LUMO is primarily localized in the electron-deficient FBT and NT regions (Fig. 6). The lowest energy singlet electronic transitions for **2-DTBFFBT** and **2-DTBFNT** are visualized through electron density difference maps.[12]

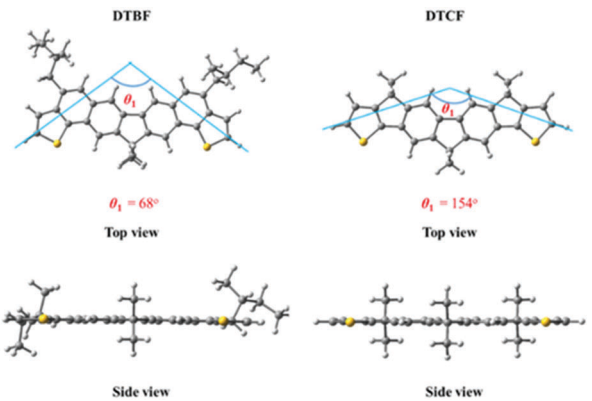

Fig. 4 Optimized geometries of **DTBF** (left) and **DTCF** (right) at the B3LYP/6-311G(d,p) level of theory. Yellow: sulfur; white: hydrogen; gray: carbon.

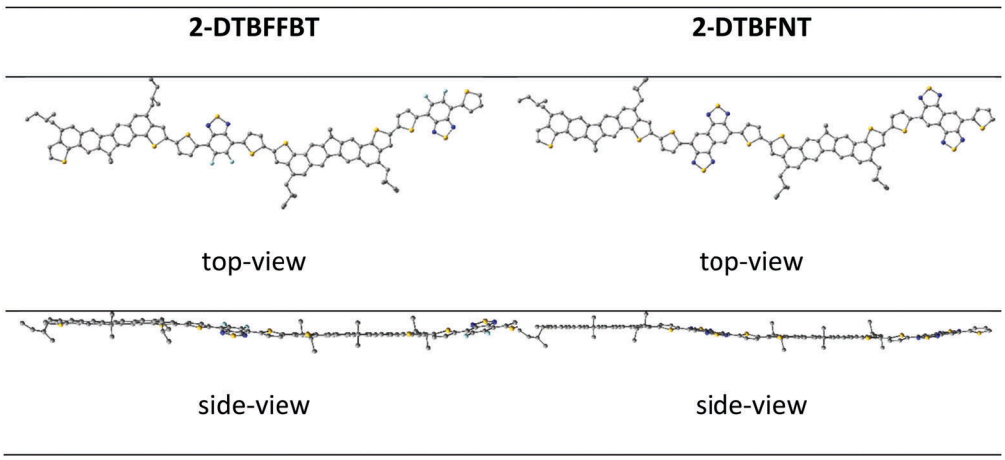

Fig. 5 Top-view (top) and side-view (bottom) images of optimized geometries of **2-DTBFFBT** and **2-DTBFNT**. Yellow: sulfur; blue: nitrogen; light blue: fluorine; gray: carbon; hydrogen atoms are omitted for clarity.

This journal is © The Royal Society of Chemistry 2016

Published on 07 November 2016. Downloaded by Synchrotron Radiation Library on 23/11/2016 03:23:59.

Table 2 Calculated[a] HOMO/LUMO energy, excitation energy, oscillator strength, and configuration (with a large CI coefficient) of the excited states

Compound	HOMO (eV)	LUMO (eV)	Excitation energy λ_{exp}[b] (nm)	λ_{calc} (nm)	Oscillator strength	Symmetry	Configurations[c]
PDTBFFBT	−5.49	−3.08	522	644	2.50	Singlet-A	H → L
			414	435	0.95	Singlet-A	H → L+2
				434	0.98	Singlet-A	H → L+2
PDTBFNT	−5.49	−3.21	626	683	2.27	Singlet-A	H → L
			400	629	0.72	Singlet-A	H → L+1
				453	0.98	Singlet-A	H → L+1
				445	1.60	Singlet-A	H → L+3

[a] TD-MPW1PW91/6-311G(d,p), PCM = $CHCl_3$. [b] Experimental values were measured in the chloroform solution. [c] Only the configuration with the largest coefficient in the CI expansion of each state is listed.

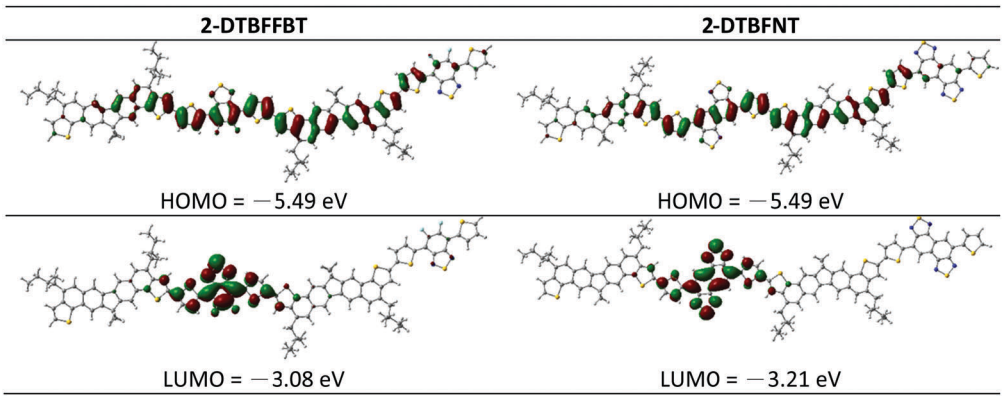

Fig. 6 The HOMO and LUMO plots (isovalue = 0.02 au) of the model compounds, **2-DTBFFBT** and **2-DTBFNT**, calculated at the level of TD-MPW1PW91/6-311G(d,p)//B3LYP/6-311G(d,p).

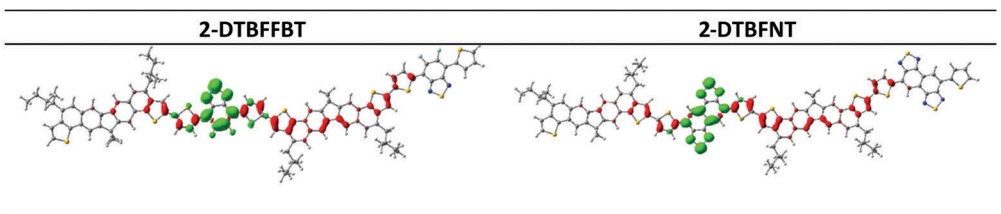

Fig. 7 Electron density difference maps (isovalue = 0.001 au) of the lowest energy singlet electronic transitions for **2-DTBFFBT** and **2-DTBFNT**. Red indicates a decrease in charge density, while green indicates an increase.

As illustrated in Fig. 7, both transitions are attributed to intramolecular charge separation between the donor (**DTBF**) and the acceptor (FBT or BT) after photo-excitation.

Photovoltaic characteristics

Bulk heterojunction solar cells with the ITO/ZnO/polymers: $PC_{71}BM/MoO_3/Ag$ configuration were fabricated and their performances were measured under a simulated AM1.5G illumination of 100 mW cm^{-2}. *J–V* curves and EQE spectra of the devices are depicted in Fig. 8 and the optimized device characteristics are summarized in Table 3.

The inverted device with the **PDTBFFBT**:$PC_{71}BM$ blend exhibited an open-circuit voltage (V_{oc}) of 0.80 V, a short-circuit current (J_{sc}) of 1.09 mA cm^{-2}, and a fill factor (FF) of 31.8%, delivering a low PCE of 0.28%. On the other hand, the device with **PDTBFNT**:$PC_{71}BM$ exhibited a V_{oc} of 0.92 V, a J_{sc} of 7.85 mA cm^{-2}, and an FF of 46.4%, delivering a PCE of 3.35%. By adding 5 vol% diphenyl ether (DPE) as an additive, the **PDTBFNT**:$PC_{71}BM$-based device showed an improved PCE of 5.22% and the PCE of the **PDTBFFBT**:$PC_{71}BM$-based device also increased to 2.68%. The performance enhancement is mainly attributed to the greater J_{sc} and the higher FF, implying that the use of DPE optimizes the morphology for better charge-carrier transportation.[13] Moreover, the much lower J_{sc} of the **PDTBFFBT**:$PC_{71}BM$ device might derive from unfavorable intermolecular charge transfer due to the higher-lying LUMO energy level of **PDTBFFBT**. It

Published on 07 November 2016. Downloaded by Synchrotron Radiation Library on 23/11/2016 03:23:59.

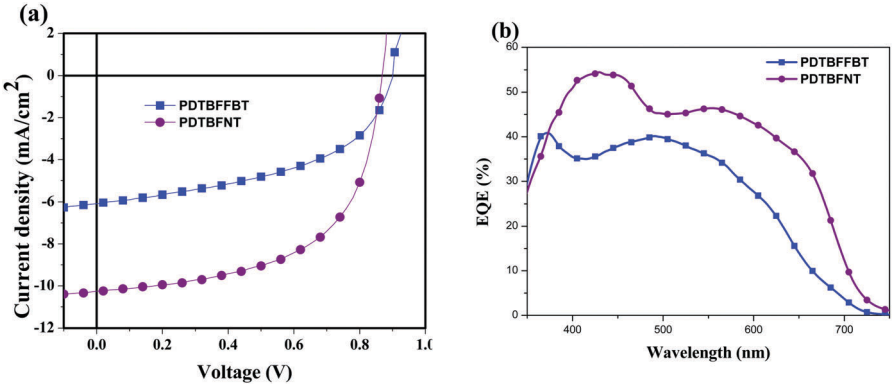

Fig. 8 (a) *J–V* characteristics of ITO/ZnO/polymers:$PC_{71}BM$/MoO_3/Ag under simulated AM1.5G illumination of 100 mW cm^{-2}, (b) the corresponding external quantum efficiency (EQE) spectra.

Table 3 Photovoltaic characteristics[a]

Device	Polymer : $PC_{71}BM$ (wt% ratio)	V_{oc} (V)	J_{sc} (mA cm^{-2})	FF (%)	PCE (%)
PDTBFFBT	1 : 2	0.80	1.09	31.8	0.28
PDTBFFBT	1 : 1.5[b]	0.90	6.08	49.0	2.68
PDTBFNT	1 : 2	0.92	7.85	46.4	3.35
PDTBFNT	1 : 2[b]	0.86	10.25	59.2	5.22

[a] The inverted device with ITO/ZnO/polymers:$PC_{71}BM$/MoO_3/Ag configuration. [b] With 5 vol% DPE additive.

is worth mentioning that both polymers exhibited high V_{oc} values up to *ca.* 0.90 V as a result of their low-lying HOMO energy levels.

GIXS measurements

The molecular stacking of the **PDTBFFBT**:$PC_{71}BM$ and **PDTBFNT**:$PC_{71}BM$ blends on the ZnO-coated ITO glass substrates was investigated by grazing-incidence X-ray scattering (GIXS). The thin films are prepared based on the optimized conditions used in the photovoltaic measurements. The 2-D GIXS images are illustrated in Fig. 9 and their corresponding 1-D diffraction patterns are plotted in Fig. 10. The peak at the scattering vector q = 1.33 Å^{-1} is assigned to the isotropically oriented fullerene clusters. The **PDTBFFBT**:$PC_{71}BM$ and **PDTBFNT**:$PC_{71}BM$ blends exhibited (h00) signals assigned to a lamellar spacing (d_1) of *ca.* 24 Å and 20 Å, respectively, corresponding to the side-chain interdigitation of the polymer. The **PDTBFNT**:$PC_{71}BM$ film exhibited an out-of-plane diffraction peak (face-on) at q_z = 1.75 Å^{-1} corresponding to the π-stacking with a distance (d_π) of *ca.* 3.58 Å. Nevertheless, the **PDTBFFBT**:$PC_{71}BM$ blend does not exhibit such a diffraction peak. The face-on alignment of conjugated polymers is beneficial for vertical charge transport in solar cell devices, which contributes to the better efficiency of the **PDTBFNT**-based device.[10c,14]

Transistor characterization

Organic field-effect transistor (OFET) mobilities of **PDTBFFBT** and **PDTBFNT** were measured by the devices using a bottom-gate/top-contact configuration with evaporated gold source/drain electrodes (40 nm in thickness). SiO_2 as a gate dielectric in the OFET devices was modified with octadecyltrichlorosilane (ODTS) to form a self-assembled monolayer (SAM). The output and transfer plots of the devices exhibited typical p-type OFET characteristics (Fig. 11). The hole mobility of the **PDTBFFBT** device is 3.96 × 10^{-3} cm^2 V^{-1} s^{-1} with an on–off ratio of 1.25 × 10^3, while that of the **PDTBFNT** device is 1.90 × 10^{-2} cm^2 V^{-1} s^{-1} with an on–off ratio of 2.22 × 10^5. (Table 4).

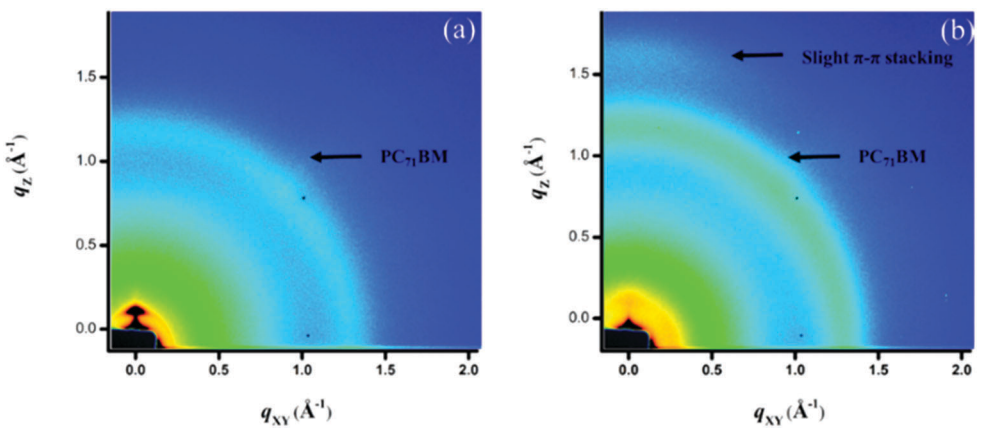

Fig. 9 2D-GIXS images of (a) **PDTBFFBT**/$PC_{71}BM$ and (b) **PDTBFNT**/$PC_{71}BM$ blend films.

 This journal is © The Royal Society of Chemistry 2016

Published on 07 November 2016. Downloaded by Synchrotron Radiation Library on 23/11/2016 03:23:59.

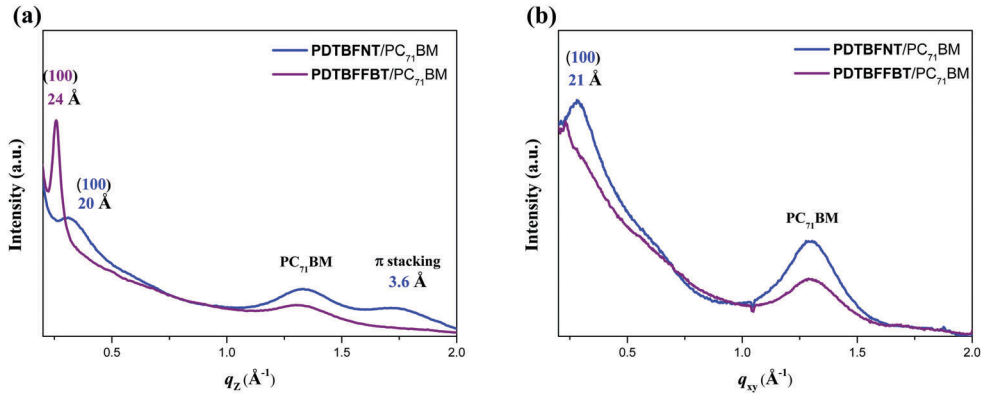

Fig. 10 1-Dimensional (a) out-of-plane and (b) in-plane GIXS profiles of (a) **PDTBFFBT**/$PC_{71}BM$ and (b) **PDTBFNT**/$PC_{71}BM$ blend films.

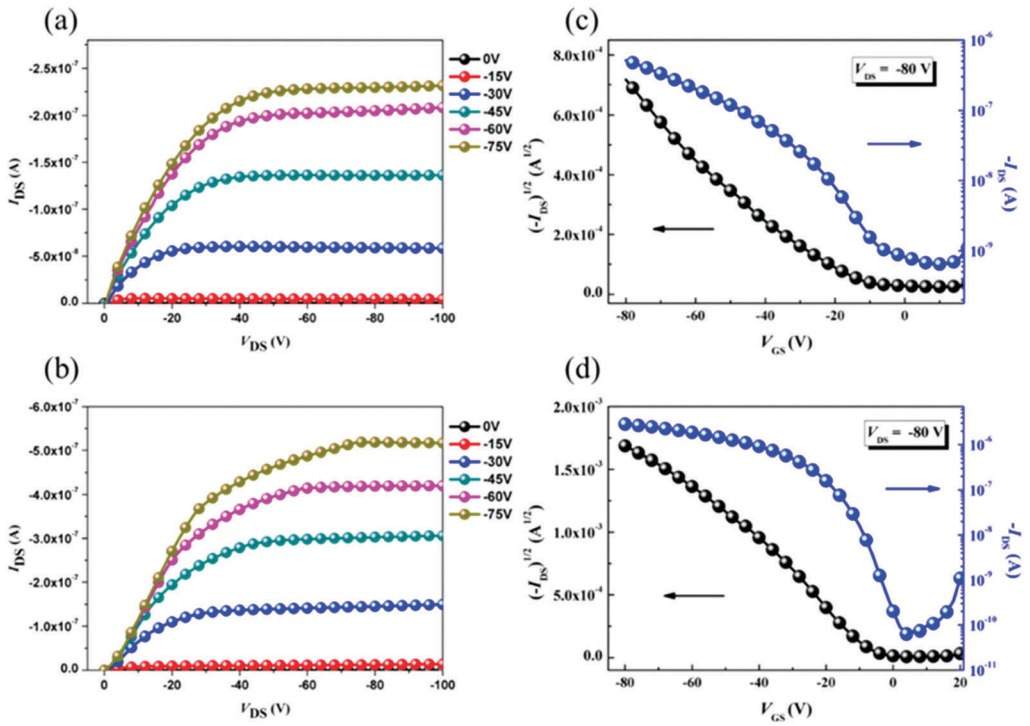

Fig. 11 Typical output curves (a and b) and transfer plots (c and d) of the bottom-gate/top-contact OFET devices for **PDTBFFBT** and **PDTBFNT**, respectively.

Table 4 Bottom-gate/top-contact OFET characteristics of polymer thin films

Polymer	SAM layer	Annealing temp (°C)	Mobility ($cm^2\ V^{-1}\ s^{-1}$)	On/off ratio	V_t (V)
PDTBFFBT	ODTS	200	3.96×10^{-3}	1.3×10^3	−29.0
PDTBFNT	ODTS	160	1.90×10^{-2}	2.2×10^5	−7.1

Conclusions

A facile synthetic route was designed to make a new ladder-type heptacyclic dithienobenzofluorene (**DTBF**) framework, where the central 2,7-fluorene unit is covalently rigidified with two outer thiophenes by two sp^2–sp^2 C═C bridges. The **DTBF** framework with two 2-octyldodecyl groups at its 5,10-positions was constructed through DBU-induced double benzannulation of a dieneyne-containing precursor **3**. In comparison with the sp^3-carbon bridged dithienocyclopentafluorene (**DTCF**) analogue, the ethylene-bridged **DTBF** possesses less steric hindrance and a more curved conjugated backbone. The rigid and coplanar **Br-DTBF** monomer was copolymerized with **Sn-DTFBT** and **Sn-DTNT** *via* Stille coupling to produce two donor–acceptor copolymers, **PDTBFFBT** and **PDTBFNT**, respectively. **PDTBFNT** has a smaller optical band gap than **PDTBFFBT**, indicating that the accepting strength of NT is stronger than that of FBT. Bulk heterojunction solar cells with the ITO/ZnO/polymers:$PC_{71}BM$/MoO_3/Ag

Published on 07 November 2016. Downloaded by Synchrotron Radiation Library on 23/11/2016 03:23:59.

configuration were fabricated and examined under a simulated AM1.5G illumination of 100 mW cm^{-2}. By adding 5 vol% DPE as an additive, the efficiencies of **PDTBFNT**-based and **PDTBFFBT**-based devices were improved to 5.22% and 2.68%, respectively. The superior efficiency of **PDTBFNT** over **PDTBFFBT** mainly comes from the higher J_{sc} and FF which are attributed to the better LUMO energy alignment between **PDTBFNT** and $PC_{71}BM$, as well as the face-on π-stacking of **PDTBFNT** for efficient vertical charge transport within the **PDTBFNT**:$PC_{71}BM$ blend. Moreover, **PDTBFNT** achieved a higher hole mobility of 1.90×10^{-2} cm^2 V^{-1} s^{-1}. It is envisaged that **DTBF** can be utilized as a useful building block to construct new semiconducting materials for organic optoelectronics.

Acknowledgements

We thank the Ministry of Science and Technology and the Ministry of Education in Taiwan for financial support. We thank the National Center of High-performance Computing (NCHC) in Taiwan for computer time and facilities. Y. J. C thanks the support from the Golden-Jade fellowship of the Kenda Foundation, Taiwan.

References

1 (*a*) S. Günes, H. Neugebauer and N. S. Sariciftci, *Chem. Rev.*, 2007, **107**, 1324–1338; (*b*) G. Yu, J. Gao, J. C. Hummelen, F. Wudl and A. J. Heeger, *Science*, 1995, **270**, 1789–1791; (*c*) J. Chen and Y. Cao, *Acc. Chem. Res.*, 2009, **42**, 1709–1718; (*d*) B. C. Thompson and J. M. J. Fréchet, *Angew. Chem., Int. Ed.*, 2008, **47**, 58–77; (*e*) Y.-Y. Lai, Y.-J. Cheng and C.-S. Hsu, *Energy Environ. Sci.*, 2014, **7**, 1866–1883; (*f*) C. Wang, H. Dong, W. Hu, Y. Liu and D. Zhu, *Chem. Rev.*, 2012, **112**, 2208–2267; (*g*) S. Allard, M. Forster, B. Souharce, H. Thiem and U. Scherf, *Angew. Chem., Int. Ed.*, 2008, **47**, 4070–4098; (*h*) X. Zhao and X. Zhan, *Chem. Soc. Rev.*, 2011, **40**, 3728–3743; (*i*) H. Kang, M. A. Uddin, C. Lee, K.-H. Kim, T. L. Nguyen, W. Lee, Y. Li, C. Wang, H. Y. Woo and B. J. Kim, *J. Am. Chem. Soc.*, 2015, **137**, 2359–2365.

2 (*a*) Y.-J. Cheng, S.-H. Yang and C.-S. Hsu, *Chem. Rev.*, 2009, **109**, 5868–5923; (*b*) H.-Y. Chen, J. Hou, S. Zhang, Y. Liang, G. Yang, Y. Yang, L. Yu, Y. Wu and G. Li, *Nat. Photonics*, 2009, **3**, 649–653; (*c*) L. Huo, S. Zhang, X. Guo, F. Xu, Y. Li and J. Hou, *Angew. Chem., Int. Ed.*, 2011, **50**, 9697–9702; (*d*) H. Zhou, L. Yang and W. You, *Macromolecules*, 2012, **45**, 607–632; (*e*) C. Duan, F. Huang and Y. Cao, *J. Mater. Chem.*, 2012, **22**, 10416–10434; (*f*) Y. Liang, Y. Wu, D. Feng, S.-T. Tsai, H.-J. Son, G. Li and L. Yu, *J. Am. Chem. Soc.*, 2009, **131**, 56–57; (*g*) M. Zhang, X. Guo, S. Zhang and J. Hou, *Adv. Mater.*, 2014, **26**, 1118–1123; (*h*) T. E. Kang, J. Choi, H.-H. Cho, S. C. Yoon and B. J. Kim, *Macromolecules*, 2016, **49**, 2096–2105; (*i*) M. B. Goldfinger, K. B. Crawford and T. M. Swager, *J. Am. Chem. Soc.*, 1997, **119**, 4578–4593; (*j*) J. Cao, L. Qian, F. Lu, J. Zhang, Y. Feng, X. Qiu, H.-L. Yip and L. Ding, *Chem. Commun.*, 2015, **51**, 11830–11833; (*k*) J. Cao, C. Zuo, B. Du, X. Qiu and L. Ding, *Chem. Commun.*, 2015, **51**, 12122–12125; (*l*) D. He, L. Qian and L. Ding, *Polym. Chem.*, 2016, **7**, 2329–2332; (*m*) J. Cao, L. Qian and L. Ding, *Polym. Chem.*, 2016, **7**, 1027–1030.

3 (*a*) J.-S. Wu, S.-W. Cheng, Y.-J. Cheng and C.-S. Hsu, *Chem. Soc. Rev.*, 2015, **44**, 1113–1154; (*b*) J. Cao, Q. Liao, X. Du, J. Chen, Z. Xiao, Q. Zuo and L. Ding, *Energy Environ. Sci.*, 2013, **6**, 3224–3228; (*c*) J.-S. Wu, Y.-Y. Lai, Y.-J. Cheng, C.-Y. Chang, C.-L. Wang and C.-S. Hsu, *Adv. Energy Mater.*, 2013, **3**, 457–465; (*d*) Y.-J. Cheng, J.-S. Wu, P.-I. Shih, C.-Y. Chang, P.-C. Jwo, W.-S. Kao and C.-S. Hsu, *Chem. Mater.*, 2011, **23**, 2361–2369; (*e*) H.-H. Chang, C.-E. Tsai, Y.-Y. Lai, D.-Y. Chiou, S.-L. Hsu, C.-S. Hsu and Y.-J. Cheng, *Macromolecules*, 2012, **45**, 9282–9291; (*f*) Y.-L. Chen, C.-Y. Chang, Y.-J. Cheng and C.-S. Hsu, *Chem. Mater.*, 2012, **24**, 3964–3971; (*g*) Y.-J. Cheng, S.-W. Cheng, C.-Y. Chang, W.-S. Kao, M.-H. Liao and C.-S. Hsu, *Chem. Commun.*, 2012, **48**, 3203–3205; (*h*) J.-S. Wu, Y.-J. Cheng, T.-Y. Lin, C.-Y. Chang, P.-I. Shih and C.-S. Hsu, *Adv. Funct. Mater.*, 2012, **22**, 1711–1722; (*i*) L. Qian, J. Cao and L. Ding, *J. Mater. Chem. A*, 2015, **3**, 24211–24214.

4 (*a*) F. He, W. Wang, W. Chen, T. Xu, S. B. Darling, J. Strzalka, Y. Liu and L. Yu, *J. Am. Chem. Soc.*, 2011, **133**, 3284–3287; (*b*) I. Osaka, T. Abe, M. Shimawaki, T. Koganezawa and K. Takimiya, *ACS Macro Lett.*, 2012, **1**, 437–440; (*c*) Q. Zheng, B. J. Jung, J. Sun and H. E. Katz, *J. Am. Chem. Soc.*, 2010, **132**, 5394–5404; (*d*) N. S. Baek, S. K. Hau, H.-L. Yip, O. Acton, K.-S. Chen and A. K. Y. Jen, *Chem. Mater.*, 2008, **20**, 5734–5736.

5 (*a*) Y. Li, J. Ding, M. Day, Y. Tao, J. Lu and M. D'Iorio, *Chem. Mater.*, 2004, **16**, 2165–2173; (*b*) M. Ranger, D. Rondeau and M. Leclerc, *Macromolecules*, 1997, **30**, 7686–7691; (*c*) D. Marsitzky, M. Klapper and K. Müllen, *Macromolecules*, 1999, **32**, 8685–8688; (*d*) J. Yang, C. Jiang, Y. Zhang, R. Yang, W. Yang, Q. Hou and Y. Cao, *Macromolecules*, 2004, **37**, 1211–1218; (*e*) S. H. Lee, T. Nakamura and T. Tsutsui, *Org. Lett.*, 2001, **3**, 2005–2007; (*f*) U. Scherf and E. J. W. List, *Adv. Mater.*, 2002, **14**, 477–487.

6 (*a*) J. Jacob, S. Sax, T. Piok, E. J. W. List, A. C. Grimsdale and K. Müllen, *J. Am. Chem. Soc.*, 2004, **126**, 6987–6995; (*b*) C.-H. Lee, Y.-Y. Lai, S.-W. Cheng and Y.-J. Cheng, *Org. Lett.*, 2014, **16**, 936–939; (*c*) C.-Y. Chang, Y.-J. Cheng, S.-H. Hung, J.-S. Wu, W.-S. Kao, C.-H. Lee and C.-S. Hsu, *Adv. Mater.*, 2012, **24**, 549–553; (*d*) J.-S. Wu, Y.-J. Cheng, M. Dubosc, C.-H. Hsieh, C.-Y. Chang and C.-S. Hsu, *Chem. Commun.*, 2010, **46**, 3259–3261; (*e*) Q. Zheng, B. J. Jung, J. Sun and H. E. Katz, *J. Am. Chem. Soc.*, 2010, **132**, 5394–5404; (*f*) M. Wang, H. Qin, L. Wang, J. Wei, D. Cai, Z. Yin, Y. Ma, S.-C. Chen, C. Tang and Q. Zheng, *J. Mater. Chem. A*, 2015, **3**, 21672–21681; (*g*) L. Wang, D. Cai, C. Tang, M. Wang, Z. Yin and Q. Zheng, *J. Mater. Chem. C*, 2015, **3**, 5631–5641; (*h*) Q. Tu, D. Cai, L. Wang, J. Wei, Q. Shang, S.-C. Chen, Y. Ma, Z. Yin, C. Tang and Q. Zheng, *J. Mater. Chem. C*, 2016, **4**, 6160–6168.

7 (*a*) L. H. Slooff, S. C. Veenstra, J. M. Kroon, D. J. D. Moet, J. Sweelssen and M. M. Koetse, *Appl. Phys. Lett.*, 2007, **90**, 143506; (*b*) F. Zhang, K. G. Jespersen, C. Björström, M. Svensson, M. R. Andersson, V. Sundström, K. Magnusson, E. Moons, A. Yartsev and O. Inganäs, *Adv. Funct. Mater.*, 2006,

 This journal is © The Royal Society of Chemistry 2016

Published on 07 November 2016. Downloaded by Synchrotron Radiation Library on 23/11/2016 03:23:59.

16, 667–674; (*c*) Q. Zhou, Q. Hou, L. Zheng, X. Deng, G. Yu and Y. Cao, *Appl. Phys. Lett.*, 2004, **84**, 1653–1655; (*d*) M. Svensson, F. Zhang, S. C. Veenstra, W. J. H. Verhees, J. C. Hummelen, J. M. Kroon, O. Inganäs and M. R. Andersson, *Adv. Mater.*, 2003, **15**, 988–991.

8 (*a*) J. Xu, Y. Wang and D. J. Burton, *Org. Lett.*, 2006, **8**, 2555–2558; (*b*) Y. Wang and D. J. Burton, *Org. Lett.*, 2006, **8**, 5295–5298; (*c*) C. Dou, S. Saito, L. Gao, N. Matsumoto, T. Karasawa, H. Zhang, A. Fukazawa and S. Yamaguchi, *Org. Lett.*, 2013, **15**, 80–83; (*d*) S.-W. Cheng, D.-Y. Chiou, Y.-Y. Lai, R.-H. Yu, C.-H. Lee and Y.-J. Cheng, *Org. Lett.*, 2013, **15**, 5338–5341; (*e*) Y.-Y. Lai, H.-H. Chang, Y.-Y. Lai, W.-W. Liang, C.-E. Tsai and Y.-J. Cheng, *Macromolecules*, 2015, **48**, 6994–7006; (*f*) Y. L. Chen, J. Y. Hsu, F. Y. Lin, Y. Y. Lai, H. C. Chou and Y. J. Cheng, *J. Org. Chem.*, 2016, **81**, 2534–2542.

9 (*a*) Y. Liu, J. Zhao, Z. Li, C. Mu, W. Ma, H. Hu, K. Jiang, H. Lin, H. Ade and H. Yan, *Nat. Commun.*, 2014, **5**, 5293; (*b*) J. Zhao, Y. Li, G. Yang, K. Jiang, H. Lin, H. Ade, W. Ma and H. Yan, *Nat. Energy*, 2016, **1**, 15027; (*c*) S.-W. Cheng, C.-E. Tsai, W.-W. Liang, Y.-L. Chen, F.-Y. Cao, C.-S. Hsu and Y.-J. Cheng, *Macromolecules*, 2015, **48**, 2030–2038.

10 (*a*) I. Osaka, M. Shimawaki, H. Mori, I. Doi, E. Miyazaki, T. Koganezawa and K. Takimiya, *J. Am. Chem. Soc.*, 2012, **134**, 3498–3507; (*b*) T. Yang, M. Wang, C. Duan, X. Hu, L. Huang, J. Peng, F. Huang and X. Gong, *Energy Environ. Sci.*, 2012, **5**, 8208–8214; (*c*) V. Vohra, K. Kawashima, T. Kakara, T. Koganezawa, I. Osaka, K. Takimiya and H. Murata, *Nat. Photonics*, 2015, **9**, 403–408; (*d*) M. Wang, X. Hu, P. Liu, W. Li, X. Gong, F. Huang and Y. Cao, *J. Am. Chem. Soc.*, 2011, **133**, 9638–9641.

11 H. Zhong, Y. Han, J. Shaw, T. D. Anthopoulos and M. Heeney, *Macromolecules*, 2015, **48**, 5605–5613.

12 N. M. O'Boyle, A. L. Tenderholt and K. M. Langner, *J. Comput. Chem.*, 2008, **29**, 839–845.

13 (*a*) H. Choi, S.-J. Ko, T. Kim, P.-O. Morin, B. Walker, B. H. Lee, M. Leclerc, J. Y. Kim and A. J. Heeger, *Adv. Mater.*, 2015, **27**, 3318–3324; (*b*) Y. Kim, H. R. Yeom, J. Y. Kim and C. Yang, *Energy Environ. Sci.*, 2013, **6**, 1909–1916.

14 X. Guo, N. Zhou, S. J. Lou, J. Smith, D. B. Tice, J. W. Hennek, R. P. Ortiz, J. T. L. Navarrete, S. Li, J. Strzalka, L. X. Chen, R. P. H. Chang, A. Facchetti and T. J. Marks, *Nat. Photonics*, 2013, **7**, 825–833.